J Appl Electrochem (2011) 41:383–388
DOI 10.1007/s10800-010-0247-y

ORIGINAL PAPER

# Inhibiting effect of cerium ions on corrosion of 3003 aluminum alloy in ethylene glycol–water solutions

**Y. Liu · Y. F. Cheng**

Received: 2 April 2010 / Accepted: 21 November 2010 / Published online: 3 December 2010


**Abstract** In this study, the inhibiting effect of cerium ions ($Ce^{3+}$) on corrosion of 3003 aluminum alloy (AA3003) in ethylene glycol–water solutions was investigated using a rotating cylinder electrode, simulating the hydrodynamic condition of the automotive cooling system. Electrochemical measurements and surface characterization were conducted to study the inhibiting mechanism of $Ce^{3+}$ on the Al alloy corrosion. It is found that $Ce^{3+}$ serves as a cathodic inhibitor, and inhibits effectively corrosion of AA3003 in the flowing ethylene glycol–water solutions. The inhibiting effect of $Ce^{3+}$ is resulted from the formation and deposit of Ce oxide and/or Ce hydroxide on the electrode surface. With the immersion time, the Ce deposit layer increases its thickness to cover the second phase particles, eliminating the galvanic coupling effect between the second phase particles and Al alloy substrate.

**Keywords** Corrosion inhibitor · Aluminum alloy · Ethylene glycol

## 1 Introduction

Previous study conducted in Cheng's group [1–9] has demonstrated that Al alloy would experience pitting corrosion, flow-assisted corrosion and erosion-corrosion in the automotive cooling system, even in the inhibited coolant. It was reported [10, 11] that, although inhibitors have been added in the commercial coolants, i.e., ethylene glycol–water solutions, most of them are not designed for corrosion inhibition of Al alloys, but for stainless steels and copper alloys that have been the conventional materials for fabrication of the automotive heat exchangers.

The inhibitive studies against the Al alloy corrosion have so far been tested under static aqueous solutions, which are quite different from a flowing system [10, 12–15], especially the ethylene glycol–water coolants [16, 17]. In the recent 20 years, rare earth metal salts have been acknowledged as excellent inhibitors for Al alloy corrosion [18–22]. The environment-friendly property makes them favorable be used in practice, replacing some toxic organic inhibitors [18]. For example, Aldykewicz et al. [19] studied the inhibiting effect of cerium (Ce) salts for an Al–Cu alloy in chloride-containing solutions, and found that Ce ions ($Ce^{3+}$) inhibit corrosion by reducing the cathodic reaction rate. Shao et al. [20] used scanning micro-reference electrode technique to probe the potential map on a 2024 Al alloy electrode in $CeCl_3$ solution. It was found that the passive film formed Al alloy electrode was enriched in $CeO_2$ and $Ce_2O_3$, showing a high corrosion resistance. Forsyth et al. [21] studied the inhibiting effect of a combination of rare earth metals including Ce, lanthanum (La), praseodymium (Pr), which showed an excellent corrosion inhibition for 2024-73 Al alloy in aqueous chloride environments.

To date, the inhibiting effect of rare earth metal salts for Al alloy corrosion in the flowing ethylene glycol–water solution has not yet understood. In this study, the inhibiting effect of $Ce^{3+}$ on electrochemical corrosion of an AA3003 in ethylene glycol–water solutions was investigated through a rotating cylinder electrode (RCE) technique simulating the hydrodynamic condition of the automotive cooling system. Various electrochemical measurements, including corrosion potential, linear polarization resistance and electrochemical impedance spectroscopy (EIS), were

Y. Liu · Y. F. Cheng (✉)
Department of Mechanical and Manufacturing Engineering, University of Calgary, Calgary, AB T2N 1N4, Canada
e-mail: fcheng@ucalgary.ca

conducted to study the corrosion behavior of the Al alloy electrode in the presence and absence of inhibitor. The surface morphology and composition of Al alloy after electrochemical test was characterized by a scanning electrochemical microscopy (SEM) and energy-dispersive X-ray analysis (EDXA). The inhibiting mechanism of $Ce^{3+}$ on Al alloy corrosion in the flowing ethylene glycol–water solutions was analyzed.

## 2 Experimental

### 2.1 Electrode and solution

The RCE with a dimension of Φ16.5 mm × 7 mm were made of AA3003 rod bar supplied by Dana Canada Corporation, with a chemical composition (wt%): Cu 0.20, Fe 0.70, Si 0.60, Mn 1.50, Mg 0.05, Cr 0.05, Zn 0.10, Ti 0.05, and Al balance. The unexposed faces and edges of the RCE were sealed with a Teflon epoxy, leaving a working area of 3.63 $cm^2$. The working surface of the electrode was ground with 800 and 1200 grit silicon carbide papers, polished with a 1 micron alumina paste, cleaned by deionized water, and dried in air.

The base test solution was a mixture of 50% (v/v) ethylene glycol + 50% deionized water + 0.01 M NaCl solution, simulating the automotive coolant. To investigate the inhibiting effect of $Ce^{3+}$, 0.003 M $CeCl_3$ was added into the base test solution. When inhibitor was added, the base solution did not contain NaCl in order to keep the constant $Cl^-$ concentration. The pH values of the solutions before and after the inhibitor addition were about 6.41 and 6.47, respectively. All solutions were made from analytic grade reagents and ultra-pure deionized water (18 MΩ cm in resistivity).

### 2.2 Hydrodynamic simulating

During test, the rotating speed of RCE was set at 3000 rpm. The Reynolds number (Re) was determined by the geometry of the electrode, fluid flow velocity, and kinematic viscosity of the solution by [23]:

$$\mathrm{Re} = \frac{2\omega r^2}{v} \quad \text{(for RCE)} \tag{1}$$

where $\omega$ is the angular rotating velocity of RCE, $r$ is the radius of RCE, and $v$ is the kinematic viscosity of the solution ($2.03 \times 10^{-6}$ $m^2$ $s^{-1}$). At a rotating speed of 3000 rpm, Re was approximately equal to 20,000, representing a turbulent flow.

### 2.3 Electrochemical measurement

Electrochemical measurements were conducted on a three-electrode cell, where AA3003 RCE was used as working electrode (WE), a saturated calomel electrode (SCE) as reference electrode (RE), and a Pt wire as counter electrode (CE), using a Solartron 1280c electrochemical system. The IR drop compensation mode of the instrument was set at "ON" with an input value around 6,000 Ω, which was estimated through the EIS measurement.

Prior to electrochemical measurement, the Al alloy WE was immersed in the solution for 1–3 days. Linear polarization resistance measurement was then performed at the potential range of $E_{corr} \pm 25$ mV, with a potential sweep rate of 0.166 mV/s. The values of polarization resistance, corrosion current density, and corrosion potential were fitted through a PowerCORR analytical software. The EIS were measured at corrosion potential with a sinusoidal potential excitation of 20 mV (peak-to-peak) in the frequency range from $10^5$ to $10^{-3}$ Hz.

All the tests were performed at a room temperature (about 20 °C) and open to air.

### 2.4 Surface characterization

After immersion for 1–3 days, the Al alloy electrode was removed from the solution, rinsed with deionized water, dried with cold air, and sent for surface analysis. The morphology of the electrode was observed with a Philips XL30 SEM. Prior to the SEM observation, a layer of gold was coated on the electrode surface to enhance the electrical conductivity. Chemical composition was determined by the combined EDXA.

## 3 Results

### 3.1 Corrosion potential measurement

Figure 1 shows the time dependence of corrosion potential of AA3003 RCE measured in the base solution in the presence and absence of 0.003 M $CeCl_3$. It is seen that the addition of $CeCl_3$ in the solution shifted $E_{corr}$ of the Al alloy RCE negatively.

### 3.2 Linear polarization resistance measurements

Figure 2 shows the linear polarization resistance of AA3003 RCE measured in the base solution with and without 0.003 M $CeCl_3$ after 3 days of immersion.

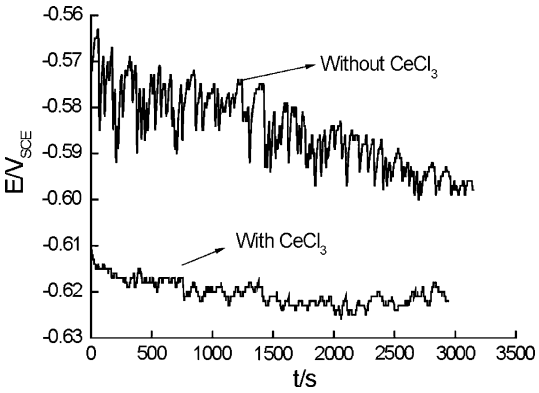


**Fig. 1** Time dependence of corrosion potential of AA3003 RCE measured in the base solution with and without 0.003 M $CeCl_3$

According to Stern and Geary model [24, 25], the polarization resistance ($R_p$) is obtained from the fitting slope (d$E$/d$i$) of the linear relationship between potential and current density:

$$R_p = \left[\frac{\Delta E}{\Delta i}\right]_{\Delta E \to 0} \quad (2)$$

The corrosion current density ($i_{corr}$) was calculated by:

$$i_{corr} = \frac{B}{R_p} \quad (3)$$

where $B$ is a proportionality constant which is usually taken as 26 mV [27].

The fitting values of $R_p$, $i_{corr}$, and $E_{corr}$ are listed in Table 1. It is seen that, in the presence of $Ce^{3+}$, the polarization resistance increased and the corrosion current density decreased, compared to those measured in the absence of $Ce^{3+}$.

### 3.3 EIS measurement

Figure 3 shows the Nyquist diagrams measured on AA3003 RCE measured in the base solution without and with 0.003 M $CeCl_3$ after 1 and 3 days of immersion. It is seen that the EIS plot measured in the absence of $CeCl_3$ was characterized with a semicircle over the whole frequency range. For RCE immersing in $CeCl_3$-containing solution for 1 day, a semicircle with the bigger size than that measured in the absence of $CeCl_3$ was observed. After 3 days of immersion in $CeCl_3$-containing solution, the EIS plot showed an overlap of two semicircles, with a further bigger size.

**Table 1** Electrochemical parameters fitted from the linear polarization resistance measurement for AA3003 RCE after 3 days of immersion in the base solution with and without 0.003 M $CeCl_3$

| Solution | $R_p$ ($\times 10^5$) ($\Omega$ cm$^2$) | $i_{corr}$ (nA cm$^{-2}$) | $E_{corr}$ (V, SCE) |
|---|---|---|---|
| Without $CeCl_3$ | 0.21 | 1220 | −0.595 |
| With $CeCl_3$ | 7.36 | 35.3 | −0.615 |

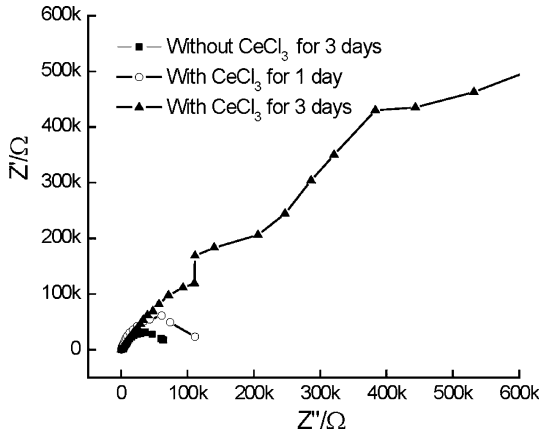


**Fig. 3** Nyquist diagram measured on AA3003 electrode in the base solution without and with 0.003 M $CeCl_3$ after 1 and 3 days of immersion

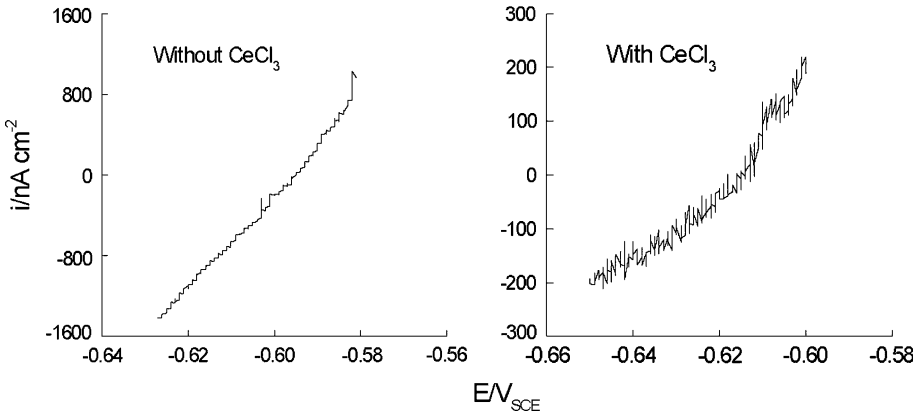


**Fig. 2** Linear polarization resistances measured on AA3003 RCE after 3 days of immersion in the base solution without and with 0.003 M $CeCl_3$

### 3.4 Surface characterization

Figure 4 shows the SEM surface morphology of AA3003 electrode after 1 day of immersion in $CeCl_3$-containing solution. A number of second phase particles shaped of a stretched ellipse with a diameter of about 5 μm were observed on Al alloy substrate. Moreover, another type of particles shaped of needles with an average length of about 1 μm was also observed. Figure 5 shows the EDX spectrum measured at the area marked in Fig. 4, where both second phase particles and the needle-shaped particles were included. It is seen that elements Fe, Mn, and Ce were detected. A comparable elemental distribution is shown in Table 2.

Figure 6 shows the SEM view of the surface morphology of AA3003 electrode after 3 days of immersion in $CeCl_3$-containing solution. It is seen that a great number of particles with radius of about 10–20 μm deposited on the electrode surface. Figure 7 shows the EDX spectrum measured at the area marked in Fig. 6, where the depositing particles were present. It is seen that, in addition to Al and O, Ce was presented in the spectra. A comparable elemental distribution is shown in Table 3.

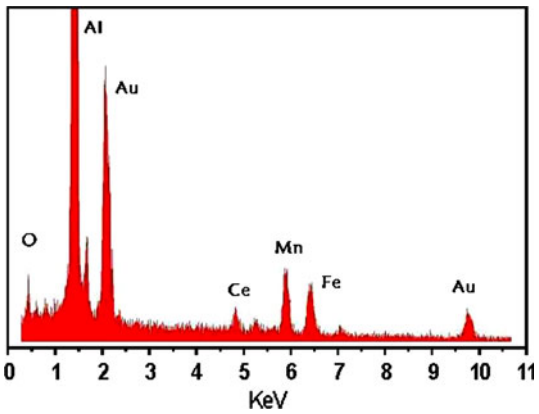


**Fig. 5** EDX spectrum obtained on AA3003 electrode at the marked area in Fig. 4

**Table 2** Elemental concentration distribution at the area marked in Fig. 4

| Elements | Al | Mn | Fe | Ce | O |
|---|---|---|---|---|---|
| wt% | 78.6 | 8.4 | 7.1 | 4.8 | 1.1 |

## 4 Discussion

This study shows that the addition of $Ce^{3+}$ would inhibit corrosion of AA3003 in the flowing, ethylene glycol–water solutions, as seen by an increasing polarization resistance and the decreasing corrosion current density in Table 1 as well as the increasing size of the semicircle, i.e., the charge-transfer resistance, in EIS plots in Fig. 3. Moreover, the corrosion potential of the Al alloy electrode is shifted negatively upon the $Ce^{3+}$ addition, indicating that $CeCl_3$ serves as a cathodic inhibitor [10]. From Fig. 1, corrosion potential of the electrode approaches a relatively steady value more rapidly than that in the absence of $Ce^{3+}$ ions. Therefore, the $Ce^{3+}$ inhibitor favors the stabilization of the electrode status. In general, an addition of inhibitor in the solution could affect the electrode state by adsorption, oxidation, or deposit mechanism. While the adsorption mechanism is usually encountered in organic inhibitors where the specific atoms, such as nitrogen and oxygen, could adsorb on the steel surface to form an adsorbing layer, the oxidation theory proposes that the reduction of the corrosion rate of a steel is through the oxidization of the steel to form an oxide film. The deposit theory involves the formation and deposit of a new product on the steel surface to reduce corrosion of the steel.

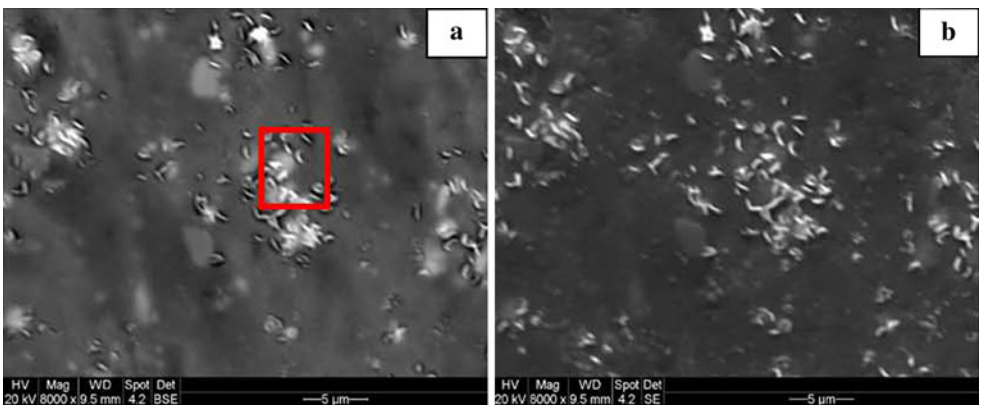


**Fig. 4** SEM views of the surface morphology of AA3003 electrode after 1 day of immersion in the base solution containing 0.003 M $CeCl_3$. **a** Backscattered SEM; **b** General SEM

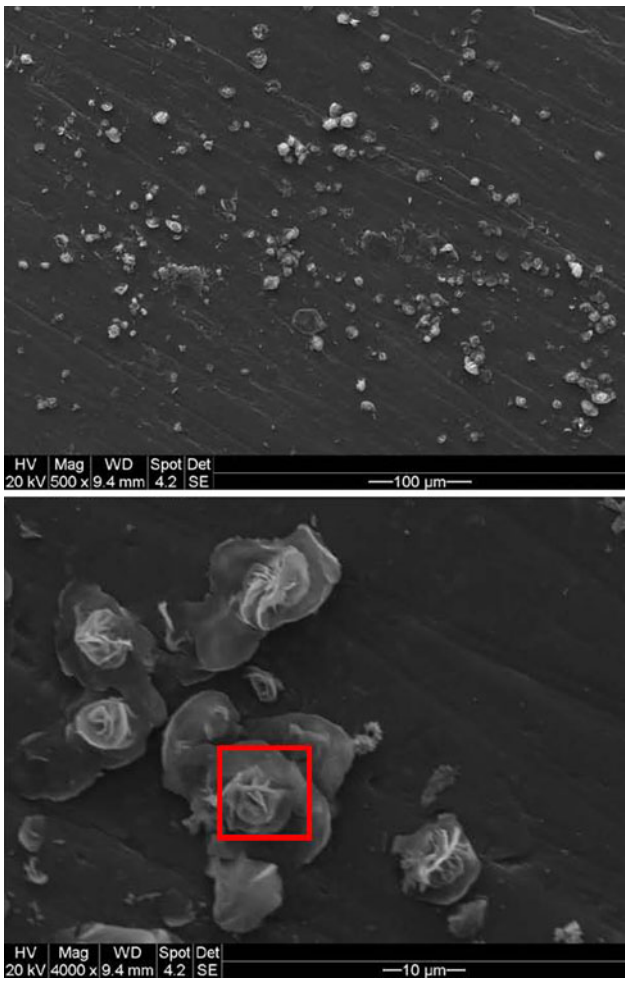


**Fig. 6** SEM views of the surface morphology of AA3003 electrode after 3 days of immersion in the base solution containing 0.003 M $CeCl_3$

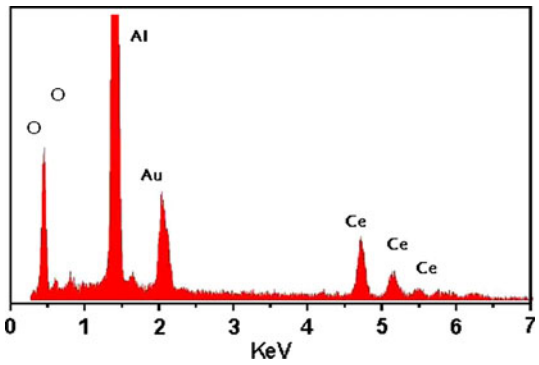


**Fig. 7** EDX spectrum obtained on AA3003 electrode at the marked area in Fig. 6

After 3 days of immersion of the Al alloy electrode in the $Ce^{3+}$-containing solution, the impedance plot is featured with two overlapped semicircles (Fig. 3). Apparently, a new interfacial reaction process is introduced. The adsorbing film mechanism is not considered because the added inhibitor does not include the specific adsorbing atoms. Moreover, the growth of adsorbing film with time does not generate new time constant, i.e., one more semicircle after 3 days of immersion, in EIS plot. Furthermore, the addition of $Ce^{3+}$ ions in the solution would not enhance the oxidation of the steel. Thus, the oxide film mechanism would not apply for the inhibition in this study.

**Table 3** Elemental concentration distribution at the area marked in Fig. 6

| Elements | Al | Ce | O |
|---|---|---|---|
| wt% | 59.0 | 20.9 | 20.1 |

The stretched second phase particles identified in Al alloy substrate (Fig. 4) are primarily $Al_x$(Fe, Mn) intermetallics, as characterized by previous study [8] as well as the high content of Mn in EDX results in Fig. 5 and Table 2. It has been acknowledged [8, 26, 27] that the Mn-enriched second phase particles forms a galvanic effect relative to the adjacent Al alloy substrate, where the particles serve as cathode and the Al alloy substrate as anode. Cathodic reactions occurring at second phase particles are dominated by the reduction of oxygen:

$$O_2 + 2H_2O + 4e^- \rightarrow 4OH^- \quad (4)$$

The $Ce^{3+}$ containing in the solution would react with hydroxide ions to form Ce oxide or Ce hydroxide depositing on the electrode surface [19–22]:

$$Ce^{3+} + 3OH^- \rightarrow Ce(OH)_3 \quad (5)$$

$$Ce(OH)_3 + OH^- \rightarrow CeO_2 + 2H_2O + e \quad (6)$$

Therefore, the depositing needle-shaped particles enriched in Ce in Figs. 4 and 6 are primarily Ce oxide or Ce hydroxide, as demonstrated by the EDX spectra in Figs. 5 and 7. The inhibiting effect of $Ce^{3+}$ is thus resulted from the formation and deposit of Ce oxide and/or Ce hydroxide on the electrode surface to affect the cathodic reaction process, and the high-frequency semicircle existing in the EIS plot measured after 3 days of immersion of the electrode is associated with the formation Ce oxide or Ce hydroxide. Furthermore, there is no Fe and Mn detected in Ce-enriched particles after 3 days of immersion (Fig. 7), which means that the Ce deposit layer is sufficiently thick to cover the second phase particles, eliminating the galvanic coupling effect between the second phase particles and Al alloy substrate. Consequently, the corrosion of Al alloy is inhibited remarkably. It is worthy pointing out that the inhibition mechanism of $Ce^{3+}$ salts applies not only on AA3003 in this study, but on other Al alloys.

## 5 Conclusions

As a cathodic inhibitor, $Ce^{3+}$ inhibits effectively corrosion of AA3003 in the flowing ethylene glycol–water solutions. The inhibiting effect of $Ce^{3+}$ is resulted from the formation and deposit of Ce oxide and/or Ce hydroxide on the electrode surface to affect the cathodic reaction process. With the immersion time, the Ce deposit layer is sufficiently thick to cover the second phase particles, eliminating the galvanic coupling effect between the second phase particles and Al alloy substrate. Consequently, the corrosion of Al alloy is inhibited remarkably.

**Acknowledgments** This study was supported by Canada Research Chairs Program, Natural Science and Engineering Research Council of Canada (NSERC) and Dana Canada Corporation.

## References

1. Niu L, Cheng YF (2008) Wear 265:367
2. Niu L, Cheng YF (2009) Corros Eng Sci Techno 44:389
3. Niu L, Cheng YF (2007) J Mater Sci 42:8613
4. Xu LY, Cheng YF (2008) Corros Sci 50:2094
5. Zhang GA, Xu LY, Cheng YF (2009) Corros Sci 51:283
6. Liu Y, Cheng YF (2009) J Appl Electrochem 39:1267
7. Xu LY, Cheng YF (2009) Corros Sci 51:2330
8. Liu Y, Cheng YF (2010) Mater Corros 61:211
9. Liu Y, Cheng YF (2010) Mater Corros 21:574
10. Nathan CC (1981) Corrosion inhibitors, NACE. Houston, Texas, US
11. Cessna JC (1964) Mater Prot 3:5
12. Davis JR (2000) Corrosion of aluminum and aluminum alloys. ASM International, Materials Park, US
13. Raspini IA (1993) Corros 49:821
14. Twiss SB, Guttenplan JD (1957) Corros 12:311
15. Thomas JGN, Treacy G, Carrol WM (1994) Corros Sci 36:11
16. Abd-El-Nabey BA, Khalil N, Khamis E (1985) Corros Sci 25:225
17. Zaharieva J, Milanova M, Mitov M, Lutov L, Manev S, Todorovsky D (2009) J Alloys Comp 470:397
18. Hiton BRW (1992) J Alloys Comp 180:15
19. Aldykewicz AJ Jr, Isaacs HS, Davenport AJ (1995) J Electrochem Soc 142:3342
20. Shao M, Huang R, Fu Y, Lin C (2002) J Rare Earths 20:640
21. Forsyth M, Markley T, Ho D, Deacon GB, Junk P, Hinton PB, Hughes A (2008) Corros 64:191
22. Tjong SC, Huo HW (2009) J Mater Eng Perf 18:88
23. Kear G, Barker BD, Stokes KR, Walsh FC (2007) Electrochim Acta 52:1889
24. Stern M, Geary AL (1957) J Electrochem Soc 104:56
25. Stern M, Geary AL (1958) J Electrochem Soc 105:638
26. Moore KL, Sykes JM, Hogg SC, Grant PS (2008) Corros Sci 50:3221
27. Barbucci A, Cerisola G, Bruzzone G, Saccone A (1997) Electrochim Acta 42:2369